Chinese J. Chem. Eng., 11 (2) 181 – 184 (2003)

Study on the Phase Behavior of Coating Matrix in Supercritical or Sub-critical Carbon Dioxide*

CAO Weiliang(曹维良), XU Jinlong(徐金龙) and ZHANG Jingchang(张敬畅)**
Faculty of Science, Beijing University of Chemical Technology, Beijing 100029, China

Abstract The high-pressure phase behavior of coating-solvent-supercritical or sub-critical carbon dioxide system was investigated experimentally. The coating matrix used was 108-acrylic resin at concentration ranging from 10% to 50% (by mass) in mixtures with *n*-butyl acetate. The experiments were conducted in a high-pressure view cell for temperatures from 35°C to 65°C and for pressures from 3.0 MPa to 8.0 MPa. The effect of temperature, pressure and content of every component on the phase behavior of the systems was observed. Finally, the ternary phase diagram for resin-solvent-CO_2 was plotted.
Keywords phase behavior, supercritical CO_2, coating matrix

1 INTRODUCTION

Supercritical fluid (SCF) technology has been paid widespread attention[1–4] in such diverse areas as separation of specialty chemicals, chemical reactions including supercritical water oxidation[5], material processing[6] and waste treatment processes[7–10].

Recently, a new "clean" technology for spraying paints has been developed which reduces emissions of volatile organic compounds (VOC) that cause ozone depletion, only by replacing the VOC with supercritical carbon dioxide, an environmentally compatible gas. This new process has the potential for reducing emissions of VOC's from the spraying of paints by up to 80%. The knowledge of the high-pressure phase behavior of coating matrix-solvent-supercritical carbon dioxide would be required to reformulate paints and other coatings. Unfortunately, there are few data in the literature on these systems, particularly for the range of concentrations being used in commercial applications.

To the best of our knowledge, there are few previously published data about thermodynamic phase behavior in the system of coating matrix-solvent-supercritical carbon dioxide[11–12]. We choose 108-acrylic resin and *n*-butyl acetate that is commercially used in coating industry as the materials for experiments. The results of a systematic series of experiments about coating matrix-solvent-supercritical carbon dioxide are presented, and the ternary phase diagram for resin-sovent-CO_2 is also constructed, which provides a theoretical basis for supercritical spraying in coating applications.

2 EXPERIMENTAL

2.1 Experimental apparatus

The observation of phase behavior of coating matrix solutions was performed by an experimental apparatus equipped with variable-volume view cell. To observe phase behavior under SCF conditions a variable-volume viewing cell is set inside the thermostatic bath. The viewing cell is equipped with a movable piston, which enables the pressure to be altered without changing the composition of the fluid inside the view cell. The internal volume of the cell is 31.875 cm^3 (working volume).

The experimental apparatus used in this work is represented in Fig. 1. The view cell contains two quartz glass windows. The temperature of water bath is controlled by a 7151-DM temperature controller (±0.05 K, Shanghai Medical Instrumental Plant). The pressure in the cell was measured by a pressure transducer(±0.03 MPa, Hangtong Inc.), and displayed by a XMZ-106 Digital Display Meter (±0.01 MPa).

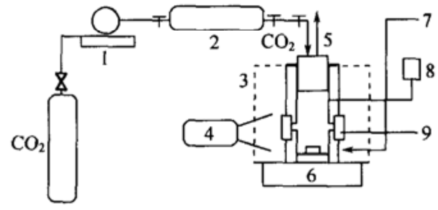

Figure 1 Schematic diagram of experimental apparatus
1—pump; 2—metering fixture; 3—thermostatic bath; 4—light source; 5—piston; 6—magnetic stirrer; 7—resin/solvent; 8—pressure gauge; 9—sight glass

2.2 Experimental materials

108-acrylic resin was selected as coating matrix material for investigation and the general characteristics of the starting sample are summarized in Table 1. The coating matrix material was supplied by Beijing Red Lion Tianyu Coatings Co., Ltd. Bone-dry

Received 2002-01-22, accepted 2002-09-12.
* Supported by the Natural Science Foundation of Beijing(No. 2992015), the National Natural Science Foundation of China(No. 20076004) and the Research Fund for the Doctoral Program of Higher Education(No. 2000001005).
** To whom correspondence should be addressed.

Table 1 General characteristics of coating matrix investigated

	M_n	M_w	M_p	M_Z	M_{Z+1}	Polydispersity
108 resin	13744	32167	27445	64736	117042	2.373063

carbon dioxide (> 99.995%) was used as the received, and supplied by Beijing Analytical Instrument Plant. The solvent, *n*-butyl acetate (AR, ⩾ 99.0%), was supplied by Tianjin Tiantai Chemical Reagent Plant.

2.3 Experimental procedure

A typical experiment is conducted in the following manner: charge the known mass mixture of coating matrix and solvent with constant composition; briefly vacuum the cell to remove air; charge a known mass of CO_2 with ±0.1 g accuracy; heat the system and blend the mixture with a magnetic stirrer and keep stable for an hour. At constant temperature the piston is moved to change the pressure in the system to make the phase transit, so the data of phase transition can be obtained from the observation of air bubble point or cloud point in the system. Each air bubble point or cloud point condition was repeated three times with a reproducibility within ±0.01 MPa to ensure the accuracy.

3 RESULTS AND DISCUSSION

Effect of contents about 108-acrylic resin, solvent and CO_2 on phase behavior is first studied, and it is expressed as a *p-T* diagram. The diagram studied here has the feature similar to that of the critical curves calculated by Van Konynenburg and Scott[13], which are not the critical curves and is only a phase diagram.

3.1 Effect of CO_2 concentration on *p-T* diagram

Figure 2 and Table 2 give the results for mixtures with a 4/1 108-acrylic resin/*n*-butyl acetate ratio. The solution in Fig. 2 is studied for CO_2 concentrations of 23.13%, 29.00%, 33.06%, and 39.28%. In general, two different phase transitions are possible: from liquid (L) to vapor-liquid (VL) and from liquid (L) to liquid-liquid (LL)[14]. In the present study, only the L-VL boundaries were observed within the studied concentrations up to 33.06% CO_2. The L-VL equilibrium is sensitive to SCF concentration and as the concentration of CO_2 increases, it shifts to lower temperatures and higher pressures. While for 39.28% CO_2, there is only L-LL boundary in the *p-T* range of the experiment. The L-VL boundaries have similar slope, but there is a tendency for the slope to increase as the SCF ratio increases. For 23.13% CO_2 the slope is 0.025 MPa·℃$^{-1}$, and becomes 0.029, 0.031, and finally 0.068 MPa·℃$^{-1}$ for 39.28% CO_2.

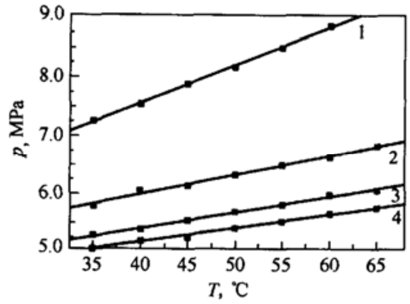

Figure 2 ***p-T* diagram for 108-acrylic resin/*n*-butyl**
concentration of CO_2, %: 1—39.28; 2—33.06; 3—29.00; 4—23.13

3.2 Effect of temperature on CO_2 solubility

The solubility of CO_2 in 108-acrylic resin (coating resin) was investigated. Fig. 3 displays the effect of temperature on the solubility for two resin solutions. The CO_2 solubility shown is normalized to 5.62 MPa. CO_2 solubility declines as temperature increases in the studied temperature range of 40—60℃. There is a turning point at 50℃, after which the CO_2 solubility declines dramatically due to the free volume difference between CO_2 and coating resin which makes CO_2 fully dissolve into the coating resin. This is not surprising since the solubility of gases in liquids generally declines as temperature increases, and it can also be interpreted by free volume theory[15]. The temperature needed to dissolve CO_2 in polymer depends on the intermolecular forces between solvent-solvent, solvent-polymer segment, and polymer segment-segment pairs in solution as given by the interchange energy, and on the free volume difference between the polymer and CO_2. The increased temperature enhances the free volume difference between CO_2 and the coating resin, so that the solubility decreases. The data in Fig. 3 also illustrate how the relative ratio of resin/solvent in a solution affects CO_2 solubility. The CO_2 solubility for 3/1 and 4/1 resin/solvent shows that as relative ratio of resin/solvent increases, the CO_2 solubility decreases. The results are expected for the co-solvent effect.

Table 2 The data about *T-p* in Fig. 2

CO_2 concentration, %	*p*, MPa						
	35.0℃	40.0℃	45.0℃	50.0℃	55.0℃	60.0℃	65.0℃
39.28	7.26	7.53	7.87	8.16	8.48	8.84	
33.06	5.79	6.05	6.12	6.31	6.49	6.62	6.81
29.00	5.29	5.38	5.53	5.67	5.80	5.96	6.05
23.13	5.04	5.19	5.24	5.39	5.51	5.64	5.74

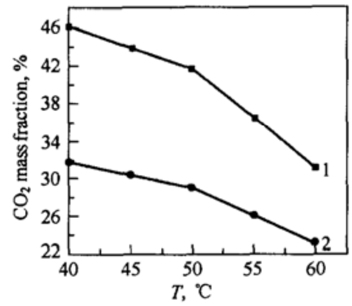

Figure 3 **Effect of temperature on CO_2 solubility**
108—resin/solvent mass ratio: 1—3/1; 2—4/1

3.3 Effect of pressure on CO_2 solubility

For resin, the qualities of solvents are related to their densities. Therefore, resin solvent quality can be finely tuned by small changes in pressure, providing a means to control solubility. Fig. 4 shows the effect of pressure on CO_2 solubility for two resin solutions with ratios of 4/1 and 3/1 resin/solvent. The CO_2 solubility shown is normalized to 65℃. It is evident that the solubility of CO_2 in the 108-acrylic resin solutions increases with pressure. Increased hydrostatic pressure reduces the free volume difference between CO_2 and resin, thus CO_2 can enter into the hole of coating matrix and act with the resin, so that the solubility increases. As shown in Fig. 4, the CO_2 solubility behaves in a similar manner under different resin/solvent ratios. From Fig. 4, we can see that the curve is in S shape. These S-shape isothermal curves can be stimulated by lattice model. This model is mainly based on the Sanchez-Lacombe (S-L) and the statistical associating fluid theory (SAFT) equation[15]. Kiszka, Wissinger and their colleagues successfully used this model to simulate some binary systems (CO_2-PMMA, ethane-LDPE).

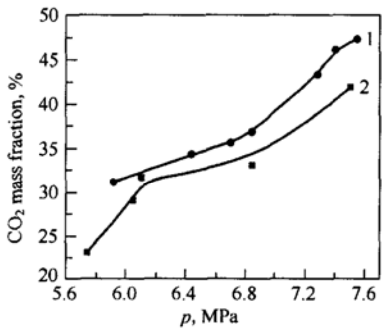

Figure 4 **Effect of pressure on CO_2 solubility**
108-resin/solvent mass ratio: 1—3/1; 2—4/1

3.4 Ternary phase diagram for acrylic-resin-*n*-butyl acetate-CO_2 system

Generally, a ternary phase diagram requires the phase equilibrium data be at constant temperature and constant pressure. Under this experimental condition, it is very difficult to obtain the data with both temperature and pressure constant. The phase equilibrium data listed in Tables 3 and 4 are the results at 50℃ and pressure close to 5.92 MPa and 6.34 MPa respectively, which were selected from a large number of experiments. The ternary phase diagram is also displayed in Fig. 5.

Table 3 **Phase equilibrium data of acrylic resin, *n*-butyl acetate and CO_2 system at 50℃ and (5.92 ± 0.05) MPa**

p, MPa	Constituent (by mass), %		
	acrylic resin	*n*-butyl acetate	CO_2
5.95	5.33	13.34	81.33
5.88	17.16	24.01	58.83
5.90	39.98	19.99	40.03
5.92	47.36	15.79	36.85
5.92	48.26	16.08	35.66
5.89	54.58	13.65	31.77
5.93	63.44	10.57	25.99
5.97	83.40	4.39	12.21

Table 4 **Phase equilibrium data of acrylic resin, *n*-butyl acetate and CO_2 system at 50℃ and (6.34 ± 0.05) MPa**

p, MPa	Constituent (by mass), %		
	acrylic resin	*n*-butyl acetate	CO_2
6.38	12.77	5.81	81.42
6.29	23.98	14.99	61.03
6.34	40.42	13.48	46.10
6.31	42.58	14.19	43.23
6.31	53.55	13.39	33.06
6.33	66.83	7.43	25.74
6.39	85.88	2.96	11.16

Figure 5 has two solubility limit curves superimposed to show how CO_2 solubility increases with pressure at temperature 50℃. Each curve divides compositions that give one-phase liquid solutions (CO_2 fully dissolved) from those that give two-phase mixtures (CO_2 exceeds solubility limit). The solubility limit curves show how the CO_2 solubility decreases as the resin level in the formulation increases. It is found from this diagram that two lines will merge together as the content of CO_2 approaches zero. While in the other side of the diagram, the two lines are distant when the content of CO_2 is almost one hundred percent. The above phenomenon is that the pressure is proportional to the content of CO_2 because the saturated vapor pressure of resin is near zero. Surprisingly, the solubility curves are found to be straight lines, which indicates, when extrapolated to the zero-solvent limit, CO_2 can have appreciable solubility in the resin at sufficiently high pressure. It is expected that the solubility curves would be curved and each would end at the pure resin corner, because CO_2 was not expected to dissolve in the resin without addition of co-solvent. This expectation was based on an analogy with hydrocarbon solvents such as hexane, which shows no solubility in the resin when active solvent is not present. From the diagram, we can see that at a pressure of 6.34 MPa, the two-phase region decreases compared with the one at the pressure of 5.92 MPa. This result is consistent with the effect of pressure on the CO_2 solubility. Spraying is normally done in the one-phase region near the solubility limit. The liquid-liquid region is avoided, because the liquid CO_2 phase extracts solvent from the resin phase. This increases viscosity and reduces the amount of solvent available to film coalescence and leveling.

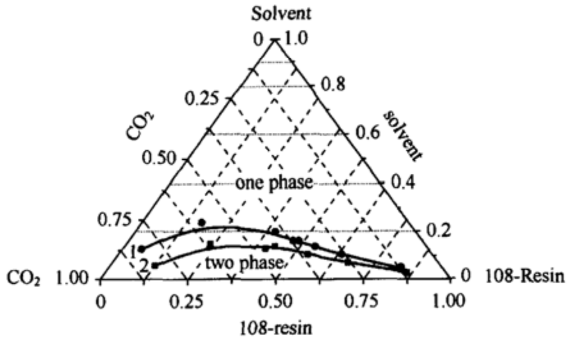

Figure 5 Ternary phase diagram for the system
p, MPa: 1—5.92±0.5; 2—6.34 ± 0.05

4 CONCLUSIONS

A systematic investigation of resin-solvent-supercritical or sub-critical CO_2 mixture phase behavior was made. This behavior is due to the large difference between the gas-like density of the CO_2 and liquid-like density of the solvent-resin binary mixture. Addition of supercritical CO_2 decreases the area of miscibility by shifting the L-LL boundary to lower temperatures and higher pressures and the L-VL boundary to higher pressures. For the effect of temperature and pressure on the CO_2 solubility, we found that the CO_2 solubility decreases as temperature increases, but increases as pressure increases at the same time. The ternary phase diagram for 108-acrylic resin, solvent and CO_2 is made, which provides the theory basis for the industrial production.

NOMENCLATURE

M_n number average of molecular weight
M_w weight average of molecular weight
M_p peak position of molecular weight
M_Z Z average of molecular weight
M_{Z+1} Z+1 average of molecular weight
p pressure, MPa
T temperature, ℃

REFERENCES

1 Zhu, H.G., Tian, Y.L., Chen, L., Qin, Y., Feng, J.J., "High-pressure phase equilibria for binary ethanol system containing supercritical CO_2", *Chinese J. Chem. Eng.*, **9** (3), 322—325 (2001).
2 Zhou, L., Zhou, Y.P., "A mathematical method for determination of absolute adsorption from experimental isotherms of supercritical gases", *Chinese J. Chem. Eng.*, **9** (1), 110—115 (2001).
3 Zhang, J.C., Wu, X.Y., Cao, W.L., "Study on critical properties for CO_2+cosolvent binary system and ternary system", *Chinese J. Chem. Eng.*, **10** (2), 223—227 (2002).
4 Li, S.F., "Solubilities of cimaterol and mabuterol in SF-CO_2", *Chinese J. Chem. Eng.*, **8** (1), 27—32 (2000).
5 Zhou, J., Wang, W.C., Zhong, C.L., "Molecular dynamics investigation of benzene in supercritical water", *Chinese J. Chem. Eng.*, **9** (2), 196—199 (2001).
6 Cai, J.G., Zhou, Z.Y., Deng, X., "Microparticle formation and crystallization rate of HMX with supercritical CO_2 antisolvent recrystallization", *Chinese J. Chem. Eng.*, **9** (3), 258—261 (2001).
7 Mark, W. R., Bartle, K. D., "SCF chromatography and extraction in surface coatings analysis-review of representative applications", *The Journal of Supercritical Fluids*, **6**, 39—49 (1993).
8 Kumar, S.K., Sutter, U.W., Reid, R.C., "Fractionation of polymers with supercritical fluids", *Fluid Phase Equilibria*, **29**, 373—382 (1987).
9 Scholsky, K.N., O'Conner, K.M., Weiss, C.S., Krukonis, V.J., "Characterization of copolymers fractionated using supercritical fluids", *J. Appl. Polym. Sci.*, **33**, 2925—2934 (1987).
10 Kabyemela, B.M., Adsciri, T., Malaluan, R.M., Arai, K., "Kinetics of glucose epimerization and decomposition in subcritical and supercritical water", *Ind. Eng. Chem. Res.*, **36** (5), 1552—1558 (1997).
11 Cao, W.L., Liu, X., Zhang, J.C., "Phase behavior of polymer-solvent-supercritical CO_2 ternary system.", *Acta Phys.-Chim. Sim.*, **17** (8), 757—760 (2001). (in Chinese)
12 Cao, W.L., Liu, X. , Zhang, J.C., "The effect of supercritical CO_2 on polymer-solvent binary system", *J. of Beijing Univ. Chem. Tech.*, **28** (4), 48—50 (2001). (in Chinese)
13 Van Konynenburg, P.H., R. L. Scott, "Critical lines and phase equilibria in binary Van Der Waals Mixtures", *Royal Society of London Philosophical Transactions*, **298**, 495—540 (1980).
14 Anastassios A. Kiamos, Marc D. Donohue, "The effect of supercritical carbon dioxide on polymer-solvent mixtures", *Macromolecules*, **27**, 357—364 (1994).
15 Christopher, F. Kirby, Mark, A. Mchugh, "Phase behavior of polymers in supercritical fluid solvents", *Chem. Rev.*, **99**, 565—602 (1999).